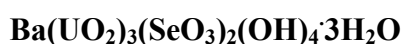




Frost, Ray L. and Cejka, Jiri and Dickfos, Marilla J. (2009) *Raman spectroscopic study of the mineral guilleminite $Ba(UO_2)_3(SeO_3)_2(OH)_4 \cdot 3H_2O$* . Journal of Raman Spectroscopy, 40(4). pp. 355-359.

© Copyright 2009 John Wiley & Sons

1 **Raman spectroscopic study of the mineral guilleminite**



3
4
5 **Ray L. Frost,^{1*} Jiří Čejka^{1,2} and Marilla J. Dickfos**

6
7 ¹ Inorganic Materials Research Program, School of Physical and Chemical Sciences,
8 Queensland University of Technology, GPO Box 2434, Brisbane Queensland 4001,
9 Australia.

10
11 ² National Museum, Václavské náměstí 68, CZ-115 79 Praha 1, Czech Republic.

12
13 **Abstract**

14
15 Raman spectrum of the mineral guilleminite Ba[(UO₂)₃O₂(SeO₃)₂](H₂O)₃ was
16 studied and complemented by the infrared spectrum of this mineral. Both spectra were
17 interpreted and compared with the spectra of marthozite, larisaite, haynesite and
18 piritite, which all should have the same phosphuranylite anion sheet topology. The
19 presence of symmetrically distinct water molecules and hydrogen bonds was inferred
20 from the spectra. This is in agreement with the crystal structural analysis of
21 guilleminite. U-O bond lengths in uranyl and O-H...O hydrogen bond lengths were
22 calculated from the Raman and/or infrared spectra of guilleminite.

23
24 **KEYWORDS:** guilleminite, uranyl selenite, Raman spectroscopy, molecular water,
25 hydrogen bonds, U-O bond length, O-H...O hydrogen bond lengths

26
27 **INTRODUCTION**

28
29 The crystal chemistry of selenium(IV) oxo-compounds shows great structural
30 versatility expressed by the great number of different compounds ¹.
31 Crystallochemical systematics of selenites was presented by Serezhkina *et al.* ².
32 Uranyl anion topology of uranyl natural and synthetic compounds inclusive uranyl
33 selenites has been elaborated by Burns ³⁻⁶. According to Finch and Murakami ⁷,

34 uranyl selenites occur where Se-bearing sulfide minerals are undergoing oxidation
35 and dissolution. Demesmaekerite, derriksite, guilleminite and marthozite are from the
36 Musonoi Cu-Co mine, near Kalwezi, Katanga Province, Democratic Republic of
37 Congo, piritite and also guilleminite from Shinkolobwe, Katanga Province,
38 Democratic Republic of Congo, haynesite and larisaitite from the Repete mine, San
39 Juan Co., Utah, U. S. A ^{8,9}.

40
41 Structures of derriksite, $\text{Cu}_4[(\text{UO}_2)(\text{SeO}_3)_2(\text{OH})_6]$, and demesmaekerite,
42 $\text{Pb}_2\text{Cu}_5[(\text{UO}_2)(\text{SeO}_3)_3]_2(\text{OH})_6(\text{H}_2\text{O})_2$, are characterized by infinite chains formed from
43 uranyl and selenite ions ^{5,10,11}, while the remaining uranyl selenite minerals,
44 guilleminite, $\text{Ba}[(\text{UO}_2)_3\text{O}_2(\text{SeO}_3)_2](\text{H}_2\text{O})_3$ ¹², marthozite, $\text{Cu}[(\text{UO}_2)_3\text{O}_2(\text{SeO}_3)_2](\text{H}_2\text{O})_8$
45 ¹³, haynesite, $[(\text{UO}_2)_3(\text{SeO}_3)_2(\text{OH})_2](\text{H}_2\text{O})_5$ ¹⁴, piritite,
46 $\text{Ca}[(\text{UO}_2)_3(\text{SeO}_3)_2(\text{OH})_4](\text{H}_2\text{O})_4$ ¹⁵, and larisaitite, $\text{Na}(\text{H}_3\text{O})[(\text{UO}_2)_3(\text{SeO}_3)_2\text{O}_2](\text{H}_2\text{O})_4$ ⁹
47 by uranyl oxo-hydroxo selenite sheets. According to Chukanov *et al.* ⁹, the general
48 formula of guilleminite, marthozite, haynesite, piritite and larisaitite is M_0 .
49 $1[(\text{UO}_2)_3(\text{SeO}_3)_2(\text{O},\text{OH})_{2-4}]_n\text{H}_2\text{O}$, where $a = 3-8$, $\text{M} = \text{M}^{2+}, 2\text{M}^+$. It is assumed that
50 these five uranyl selenite minerals may have phosphuranylite anion sheet topology
51 ^{9,16}.

52
53 Guilleminite is orthorhombic, a 7.084(1), b 7.293(1), c 16.881(4) Å, space
54 group $P2_1nm$, $Z = 2$ ¹⁷. In the crystal structure of guilleminite, there are two
55 symmetrically distinct U^{6+} in the form of uranyls, $(\text{UO}_2)^{2+}$, and one symmetrically
56 distinct Se^{4+} in the form of $(\text{SeO}_3)^{2-}$ and one symmetrically distinct Ba^{2+} . One uranyl
57 is surrounded by six equatorial oxygens thus forming a hexagonal dipyramidal uranyl
58 coordination polyhedron. The other two uranyls are surrounded by five equatorial
59 oxygens thus forming a pentagonal dipyramidal uranyl coordination polyhedra. Two
60 (UO_2O_5) pentagonal dipyramids share an edge to form a $(\text{U}_2\text{O}_4\text{O}_8)$ dimer. These
61 dimers link to form a chain of the type $(\text{U}_3\text{O}_6\text{O}_8)$ by sharing edges with UO_2O_6
62 hexagonal dipyramids. These chains are cross-linked by (SeO_3) groups and form
63 $[(\text{UO}_2)_3\text{O}_2(\text{SeO}_3)_2]$ sheets. These strongly bonded sheets are the structural units of
64 guilleminite with Ba^{2+} cations and water molecules in the interlayers. The sheets are
65 in fact linked by Ba^{2+} cations and by hydrogen bonds ¹⁷. Infrared spectra of haynesite

* Author to whom correspondence should be addressed (r.frost@qut.edu.au)

66 ¹⁸, piretite ¹⁵, larisaite ⁹ have been published. Infrared spectra of haynesite and piretite
67 were reviewed by Čejka ¹⁹. Raman and infrared spectra of haynesite ²⁰ and marthozite
68 were also presented.

69

70 The aim of this paper is the study of Raman spectra of the natural uranyl
71 selenite guilleminite, complemented by its infrared spectra. The paper is a part of
72 systematic vibrational spectroscopic research of secondary minerals formed in the
73 oxidation zone, inclusive uranyl minerals originating during hydration-oxidation
74 weathering of primary uranium minerals, such as uraninite. Raman spectroscopy was
75 proven most useful for the characterization of secondary uranyl containing minerals
76 ²⁰⁻³⁸. In order to identify and characterize the Raman and infrared spectra of
77 guilleminite, this research reports the Raman and infrared spectrum of guilleminite
78 and relates the spectra of guilleminite to the structure of the mineral.

79

80 **EXPERIMENTAL**

81

82 *Mineral*

83

84 The guilleminite mineral was obtained from the Mineralogical Research Company
85 and originated from the Musonoi Mine, Kobokobo, Congo. This sample is a 'type'
86 mineral. The chemical composition of this mineral has been published ⁸ (page 268).
87 The mineral corresponds to the formula above $\text{Ba}(\text{UO}_2)_3(\text{SeO}_3)_2(\text{OH})_4 \cdot 3\text{H}_2\text{O}$.

88

89 *Raman microprobe spectroscopy*

90

91 The crystals of marthozite were placed and orientated on the stage of an
92 Olympus BHSM microscope, equipped with 10x and 50x objectives which was part
93 of a Renishaw 1000 Raman microscope system, also including a monochromator,
94 filter system and Charge Coupled Device (CCD). Raman spectra were excited by a
95 HeNe laser (633 nm) at a resolution of 2 cm^{-1} in the range between 100 and 4000
96 cm^{-1} . Repeated acquisition using the highest magnification was accumulated to
97 improve the signal to noise ratio. Spectra were calibrated using the 520.5 cm^{-1} line of
98 a silicon wafer.

99 Spectroscopic manipulation such as baseline adjustment, smoothing and

100 normalisation were performed using the Spectracalc software package GRAMS
101 (Galactic Industries Corporation, NH, USA). Band component analysis was
102 undertaken using the Jandel 'Peakfit' software package, which enabled the type of
103 fitting function to be selected and allows specific parameters to be fixed or varied
104 accordingly. Band fitting was done using a Gauss-Lorentz cross-product function with
105 the minimum number of component bands for the fitting process. The Gauss-Lorentz
106 ratio was maintained at values greater than 0.7 and fitting was undertaken until
107 reproducible results were obtained with squared correlations of r^2 greater than 0.995.
108 Further details on the manipulation of the data has been published ^{20,22,24,28,29,32,34,38-40}
109 .

110 *Infrared spectroscopy*

111 Infrared spectra were obtained using a Nicolet Nexus 870 FTIR spectrometer
112 with a smart endurance single bounce diamond ATR cell. Spectra over the 4000–525
113 cm^{-1} range were obtained by the co-addition of 64 scans with a resolution of 4 cm^{-1}
114 and a mirror velocity of 0.6329 cm/s . Spectra were co-added to improve the signal to
115 noise ratio.

116

117 **RESULTS AND DISCUSSION**

118

119 The free linear uranyl group (UO_2)²⁺, symmetry $D_{\infty h}$, has four normal
120 vibrations, but only three fundamentals: the ν_1 symmetric stretching vibration, Raman
121 active (approximately 900-700 cm^{-1}), the ν_2 (δ) doubly degenerate bending vibration,
122 infrared active (approximately 300-200 cm^{-1}), and the ν_3 antisymmetric stretching
123 vibration, infrared active (approximately 1000-850 cm^{-1}). Distortion of the uranyl
124 group or change in the local symmetry can result in the removal of the degeneracy and
125 therefore Raman activation of the ν_2 mode and infrared activation of the ν_1 mode.

126

127 The chemistry of the selenite ion and selenite containing compounds
128 resembles the chemistry of the sulphite ion and its compounds. The symmetry of the
129 selenite ions is similar to that of sulphite, which is tetrahedral with one vacant orbital
130 thus making C_{3v} symmetry ⁴¹. The selenite ion thus has four fundamentals: the ν_1
131 symmetric stretching vibrations (approximately 790-806 or 760-855 cm^{-1}), the ν_2

132 symmetric bending vibration (approximately 430-461 cm^{-1}), the ν_3 doubly
133 degenerate antisymmetric stretching vibration (714-769 or 680-775 cm^{-1}), and the ν_4
134 doubly degenerate antisymmetric bending vibration (approximately 387-418 cm^{-1}).
135 All vibrations are Raman and infrared active [Frost et al., submitted]. The degeneracy
136 of the antisymmetric ν_3 and ν_4 modes of the $(\text{SeO}_3)^{2-}$ may be removed due to the
137 lowering of its site symmetry in the unit cell.

138

139 The Raman spectra of guillimentite in the 100 to 900 cm^{-1} region and 1400 to
140 1700 cm^{-1} are shown in Figures 1 and 2 respectively. The infrared spectra of
141 guilleminite in the 550 to 1100 cm^{-1} , 1250 to 1700 cm^{-1} and 2500 to 3750 cm^{-1} , are
142 shown in Figures 3, 4 and 5, respectively.

143

144 Raman band (infrared bands are given in parentheses) at 831 (814) cm^{-1} is
145 assigned to the $\nu_1(\text{UO}_2)^{2+}$, however, it may be also related to the $\nu_1(\text{SeO}_3)^{2-}$. No
146 Raman band was attributed to the $\nu_3(\text{UO}_2)^{2+}$. Infrared bands at 877 and 912 cm^{-1} are
147 assigned to the $\nu_3(\text{UO}_2)^{2+}$. The U-O bond lengths in uranyl may be calculated with
148 two empirical relations using wavenumbers of the stretching uranyl vibrations [$R_{\text{U-O}} =$
149 $0.575 + 106.5\nu_1^{-2/3}$ Å, and $R_{\text{U-O}} = 0.804 + 91.41\nu_3^{-2/3}$ Å, Bartlett and Cooney ⁴²,
150 Obtained calculated U-O bond lengths ($\text{Å}/\text{cm}^{-1}$) 1.780/831, 1.797/814, 1.802/877 and
151 1.776/912 are in close agreement the average U-O bond length 1.795 Å, inferred from
152 the X-ray single crystal structure of guilleminite ¹⁷. Raman band at 812 cm^{-1} was
153 assigned to the $\nu_1(\text{UO}_2)^{2+}$ in marthozite [Frost et al., submitted] and haynesite ²⁰.
154 Infrared bands at 879 and 820 cm^{-1} in the spectrum of marthozite [Frost et al.,
155 submitted] and at 898 and 815 cm^{-1} in the spectrum of piretite were attributed to the ν_3
156 $(\text{UO}_2)^{2+}$ and $\nu_1(\text{UO}_2)^{2+}$, respectively. Chukanov et al. ⁹ assigned the infrared band at
157 901 cm^{-1} in the spectrum of larisaite to the uranyl stretching vibration. Thus Raman
158 spectra of uranyl selenite minerals possessing the phosphuranylite anion sheet
159 topology are comparable in this region.

160

161 Raman band at 747 (753, 782) cm^{-1} is attributed to the $\nu_3(\text{SeO}_3)^{2-}$ vibrations.
162 Raman band at 675 (692) cm^{-1} may be related to the libration mode of water
163 molecules. Raman band at 544 cm^{-1} is probably connected with the libration mode of
164 water molecules and/or to the $\nu(\text{U-O}_{\text{ligand}})$ vibrations. Raman bands at 478 cm^{-1} and

165 345 and 419 cm^{-1} are attributed to the ν_2 and ν_4 (SeO_3)²⁻ vibrations, respectively. The
166 ν_2 (δ) (UO_2)²⁺ was observed in the Raman spectrum at 245 cm^{-1} , while the band at
167 150 cm^{-1} may be assigned to the lattice vibrations. Infrared spectrum of
168 $\text{Sr}[(\text{UO}_2)_3\text{O}_2(\text{SeO}_3)_2](\text{H}_2\text{O})_4$, observed in this region is as follows: 909 cm^{-1} (ν_3
169 (UO_2)²⁺), 865 cm^{-1} (ν_1 (UO_2)²⁺ - this interpretation is probably not correct, according
170 to the formulas $\nu_1 = 0.94\nu_3 \text{ cm}^{-1}$ and $\nu_1 = 0.89 \nu_3 + 21 \text{ cm}^{-1}$, the wavenumber of the
171 ν_1 (UO_2)²⁺ should be close to 854 or 830 cm^{-1} - for details see e.g. Čejka 1999¹⁹),
172 839, 814, 725, 615 cm^{-1} ⁴³. The structure of this synthetic compounds contains two-
173 dimensional $[(\text{UO}_2)_3(\text{O}_2)(\text{SeO}_3)_2]^{2-}$ sheets with the same phosphuranylite anion sheet
174 topology as those found in guilleminite, marthozite and larisaite, and expected also in
175 piretite and haynesite.

176

177 Infrared band at 1011 cm^{-1} is assigned to the δ UOH bending vibration. In this
178 region, infrared bands were observed in the infrared spectra of marthozite (1120,
179 1096, 1049 and 1027 cm^{-1} [Frost et al. submitted], larisaite (1044 and 1095 cm^{-1})⁹
180 and haynesite (1168, 1116, 1081 and 1036) [Čejka et al. 1999]. Chukanov et al.⁹
181 assume that some of these bands together with some other at different wavenumbers
182 may be connected with the (H_3O)⁺ bending vibrations and that especially haynesite
183 contains hydroxonium cations and may be formulated as
184 $(\text{H}_3\text{O})_2[(\text{UO}_2)_3(\text{OH})_4(\text{SeO}_3)_2]\cdot\text{H}_2\text{O}$. However, marthozite does not contain any
185 hydroxonium ions and some bands in the mentioned region may be also observed.
186 Chukanov et al.⁹ assigned a band at 1732 cm^{-1} in the infrared spectrum of haynesite
187 to the doubly degenerate bending vibration of hydroxonium ions. It is more probable
188 that this infrared band may be attributed to the combination ($\nu_1 + \nu_3$ (UO_2)²⁺) band,
189 and some bands in the region 1000-1200 cm^{-1} may be connected with the combination
190 ($\nu_1 + \nu_2$ (UO_2)²⁺ and/or ($\nu_3 + \nu_2$ (UO_2)²⁺) bands. Frost et al. did not infer the presence
191 of hydroxonium ions in the structure of haynesite in their Raman spectroscopic study
192 of the uranyl selenite mineral haynesite.²⁰

193

194 Infrared bands observed at 1403, 1424 and 1514 cm^{-1} and Raman band at 1514
195 cm^{-1} may be connected with overtones and/or combination bands. Raman band at
196 1585 cm^{-1} and two infrared bands at 1614 and 1652 cm^{-1} are assigned to the δ H_2O
197 bending vibration. Two bands observed in the infrared spectrum prove that

198 structurally nonequivalent (symmetrically distinct) water molecules are present in the
199 crystal structure of guilleminite which is in agreement with X-ray single crystal
200 structure data ¹⁷.

201

202 The ν OH stretching vibrations of water molecules are observed in the infrared
203 spectrum of guilleminite at 3552, 3463, 3293, 3082 cm^{-1} . These wavenumbers
204 correspond with O-H...O hydrogen bond lengths 3.0, 2.86, 2.75 and 2.68 Å ⁴⁴. These
205 values are close to those inferred from the X-ray single crystal structure analysis of
206 guilleminite ¹⁷.

207

208

209 **CONCLUSIONS**

210

211 Raman and infrared spectra of uranyl selenite mineral guilleminite were
212 measured, tentatively interpreted and partly compared with the spectra of marthozite,
213 larisaite, haynesite, piritite and synthetic $\text{Sr}[(\text{UO}_2)_3\text{O}_2(\text{SeO}_3)_2](\text{H}_2\text{O})_4$. All these
214 compounds should have the same phosphuranylite anion sheet topology.

215

216

217 The presence of symmetrically distinct water molecules and hydrogen bonds
218 was inferred from the spectra. Observed hydrogen bonds are in agreement with the
219 crystal structure of guilleminite. U-O bond lengths in uranyls and O-H...O hydrogen
220 bond lengths were inferred from the spectra with empirical relations by Bartlett and
221 Cooney ⁴⁵ and Libowitzky ⁴⁴, respectively.

222

223

224 **Acknowledgements**

225

226 The financial and infra-structure support of the Queensland University of
227 Technology Inorganic Materials Research Program of the School of Physical and
228 Chemical Sciences is gratefully acknowledged. The Australian Research Council
229 (ARC) is thanked for funding.

230

231

232 **References**

233

- 234 1. Koskenlinna, M. Ph. D. Thesis, Helsinki 1996.
- 235 2. Serezhkina, LB, Rastsvetaeva, RK, Serezhkin, VN. *Koord. Khim.* 1990; **16**:
236 1327.
- 237 3. Burns, PC. *Can. Miner.* 2005; **43**: 1839.
- 238 4. Burns, PC. *Mat. Res. Soc. Symposium Proc.* 2004; **802**: 89.
- 239 5. Burns, PC. *Rev. Min.* 1999; **38**: 23.
- 240 6. Burns, PC. *Am. Min.* 1997; **82**: 1176.
- 241 7. Finch, R, Murakami, T. *Rev. Min.* 1999; **38**: 91.
- 242 8. Anthony, JW, Bideaux, RA, Bladh, KW, Nichols, MC *Handbook of*
243 *Mineralogy*; Mineral Data Publishing: Tuscon, Arizona, USA, 2000; Vol. 4.
- 244 9. Chukanov, NV, Pushcharovsky, DY, Pasero, M, Merlino, S, Barinova, AV,
245 Möckel, S, Pekov, IV, Zadov, AE, Dubinchuk, VT. *Euro. J. Min.* 2004; **16**:
246 367.
- 247 10. Ginderow, D, Cesbron, F. *Act. Crys.* 1983; **C39**: 824.
- 248 11. Ginderow, D, Cesbron., F. *Act. Crys.* 1983; **C39**: 1605.
- 249 12. Cooper, MA, Hawthorne, FC. *Can. Min.* 1995; **33**: 1103.
- 250 13. Cooper, MA, Hawthorne, FC. *Can. Min.* 2001; **39**: 797.
- 251 14. Deliens, M, Piret, P. *Can. Min.* 1991; **29**: 561.
- 252 15. Vochten, R, Blaton, N, Peeters, O, Deliens, M. *Can. Min.* 1996; **34**: 1317.
- 253 16. Burns, PC. *Can. Min.* 2005; **43**: 1839.
- 254 17. Cooper, MA, Hawthorne, FC. *Can. Min.* 1995; **33**: 1103.
- 255 18. Cejka, J, Sejkora, J, Deliens, M. *Neues Jahr. Min.*, 1999: 241.
- 256 19. Cejka, J. *Rev. Min.* 1999; **38**: 521.
- 257 20. Frost, RL, Weier, ML, Reddy, BJ, Cejka, J. *J. Raman Spec.* 2006; **37**: 816.
- 258 21. Frost, RL, Dickfos, MJ. *J. Raman Spec.* 2007; **38**: 1516.
- 259 22. Frost, RL, Cejka, J. *J. Raman Spec.* 2007; **38**: 1488.
- 260 23. Locke, AJ, Martens, WN, Frost, RL. *J. Raman Spec.* 2007; **38**: 1429.
- 261 24. Frost, RL, Cejka, J, Ayoko, GA, Weier, ML. *J. Raman Spec.* 2007; **38**: 1311.
- 262 25. Frost, RL, Bouzaid, JM. *J. Raman Spec.* 2007; **38**: 873.
- 263 26. Frost, RL, Pinto, C. *J. Raman Spec.* 2007; **38**: 841.
- 264 27. Frost, RL, Weier, ML, Williams, PA, Leverett, P, Kloprogge, JT. *J. Raman*
265 *Spec.* 2007; **38**: 574.
- 266 28. Frost, RL, Cejka, J, Weier, ML. *J. Raman Spec.* 2007; **38**: 460.
- 267 29. Frost, RL, Cejka, J, Weier, ML, Martens, WN, Ayoko, GA. *J. Raman Spec.*
268 2007; **38**: 398.
- 269 30. Frost, RL, Bouzaid, JM, Martens, WN, Reddy, BJ. *J. Raman Spec.* 2007; **38**:
270 135.
- 271 31. Frost, RL, Palmer, SJ, Bouzaid, JM, Reddy, BJ. *J. Raman Spec.* 2007; **38**: 68.
- 272 32. Frost, RL, Cejka, J, Weier, M, Ayoko, GA. *J. Raman Spec.* 2006; **37**: 1362.
- 273 33. Frost, RL. *J. Raman Spec.* 2006; **37**: 910.
- 274 34. Frost, RL, Cejka, J, Weier, M, Martens, WN. *J. Raman Spec.* 2006; **37**: 879.
- 275 35. Frost, RL, Musumeci, AW, Kloprogge, JT, Adebajo, MO, Martens, WN. *J.*
276 *Raman Spec.* 2006; **37**: 733.
- 277 36. Frost, RL, Henry, DA, Weier, ML, Martens, W. *J. Raman Spec.* 2006; **37**:
278 722.
- 279 37. Frost, RL, Weier, ML, Cejka, J, Kloprogge, JT. *J. Raman Spec.* 2006; **37**: 585.
- 280 38. Frost, RL, Cejka, J, Weier, ML, Martens, W. *J. Raman Spec.* 2006; **37**: 538.

- 281 39. Frost, RL, Weier, ML, Martens, WN, Kloprogge, JT, Kristof, J. *J. Raman*
282 *Spec.* 2005; **36**: 797.
- 283 40. Frost, RL, Henry, DA, Erickson, K. *J. Raman Spec.* 2004; **35**: 255.
- 284 41. Greenwood, NN, Earnshaw, A *Chemistry of elements*; Pergamon Press:
285 Oxford 1984.
- 286 42. Bartlett, JR, Cooney, RP. *J. Mol. Struc.* 1989; **193**: 295.
- 287 43. Almond, PM, Albrecht-Schmitt, TE. *Am. Min.* 2004; **89**: 976.
- 288 44. Libowitzky, E. *Monat. Chem.* 1999; **130**: 1047.
- 289 45. Bartlett, JR, Cooney, RP. *J. Mol. Struc.* 1989; **193**: 295.
- 290
- 291
- 292
- 293

294 **List of Figures**

295

296 Figure 1 Raman spectrum of guilleminite in the 100 to 900 cm^{-1} region.

297

298 Figure 2 Raman spectrum of guilleminite in the 1400 to 1700 cm^{-1} region.

299

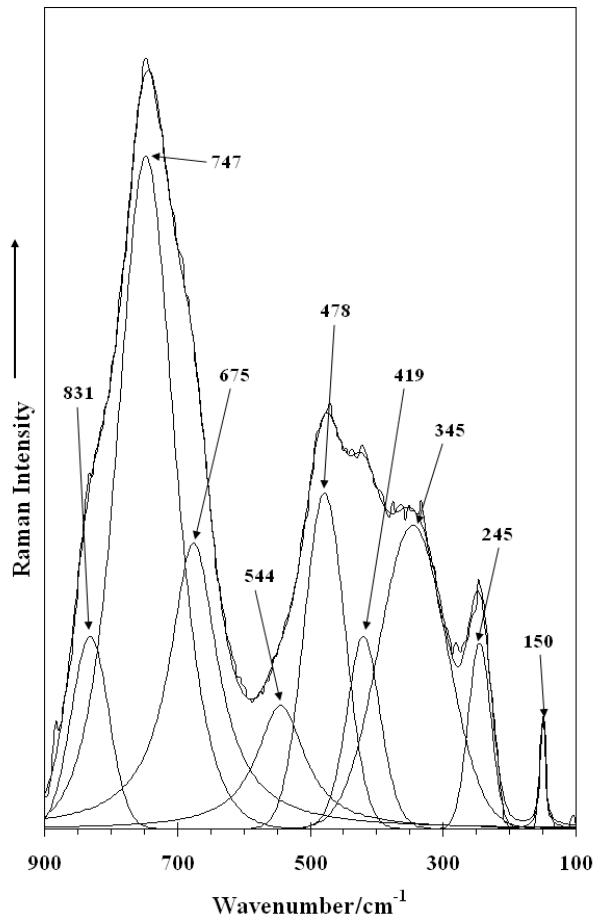
300 Figure 3 Infrared spectrum of guilleminite in the 550 to 1100 cm^{-1} region.

301

302 Figure 4 Infrared spectrum of guilleminite in the 1250 to 1650 cm^{-1} region.

303

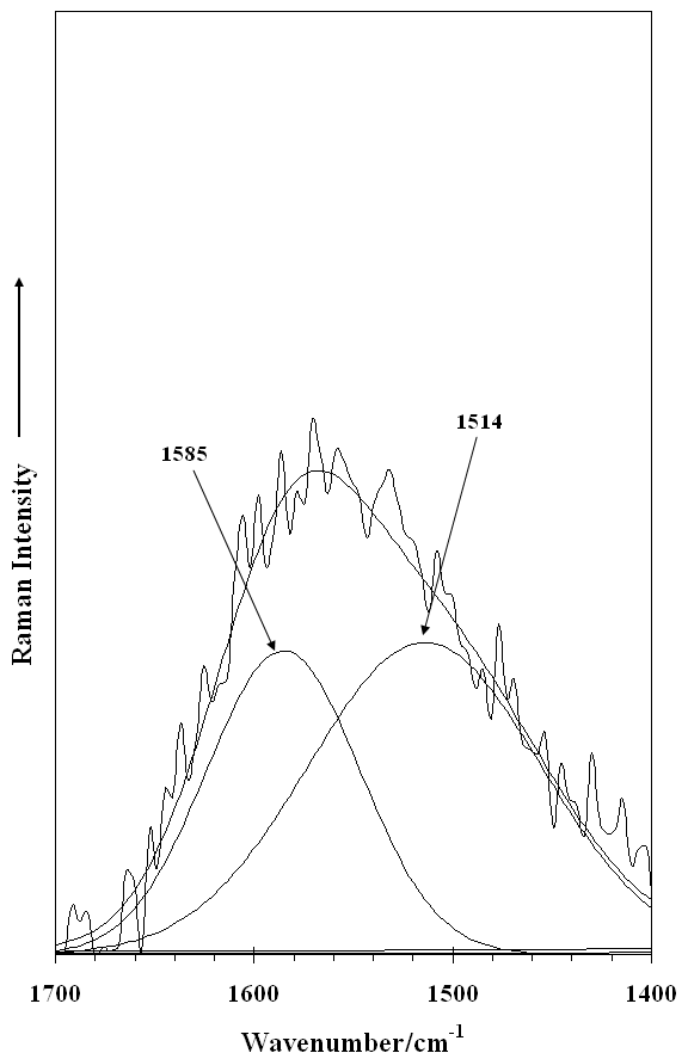
304 Figure 5 Infrared spectrum of guilleminite in the 2500 to 3700 cm^{-1} region.



305

306

307 **Figure 1**



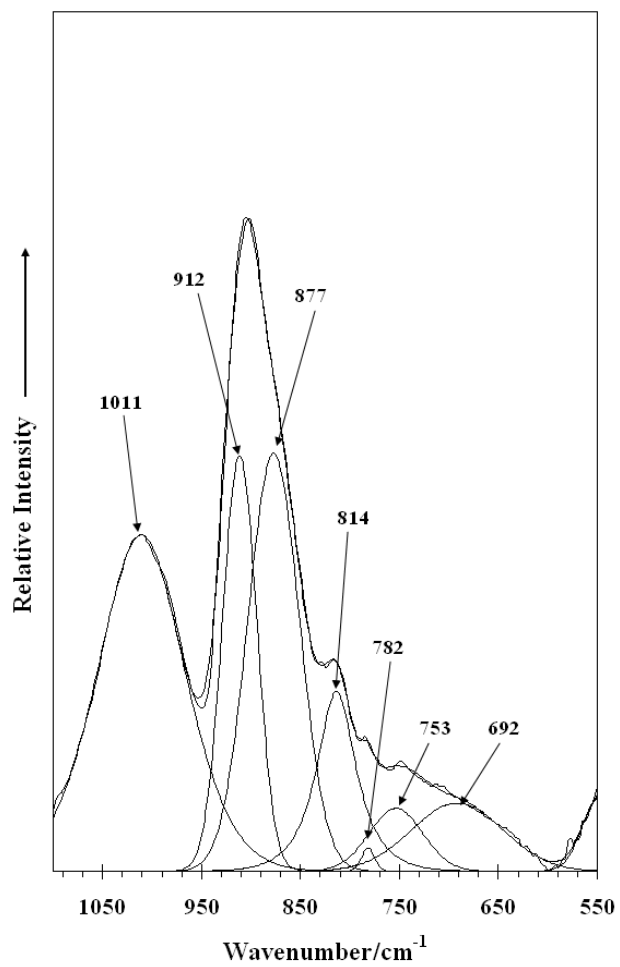
308

309

310 **Figure 2**

311

312



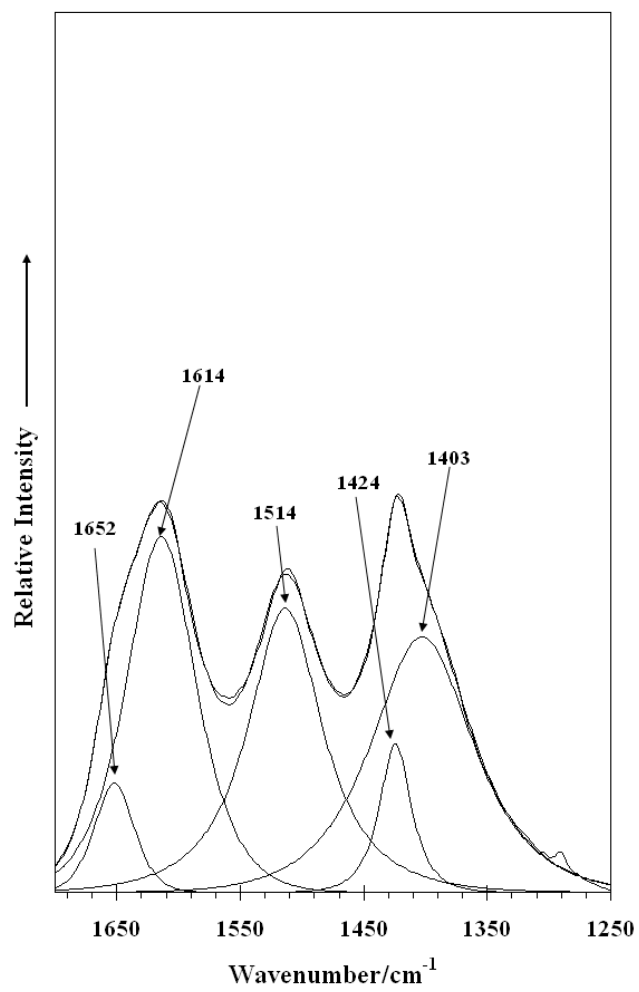
313

314

315 **Figure 3**

316

317



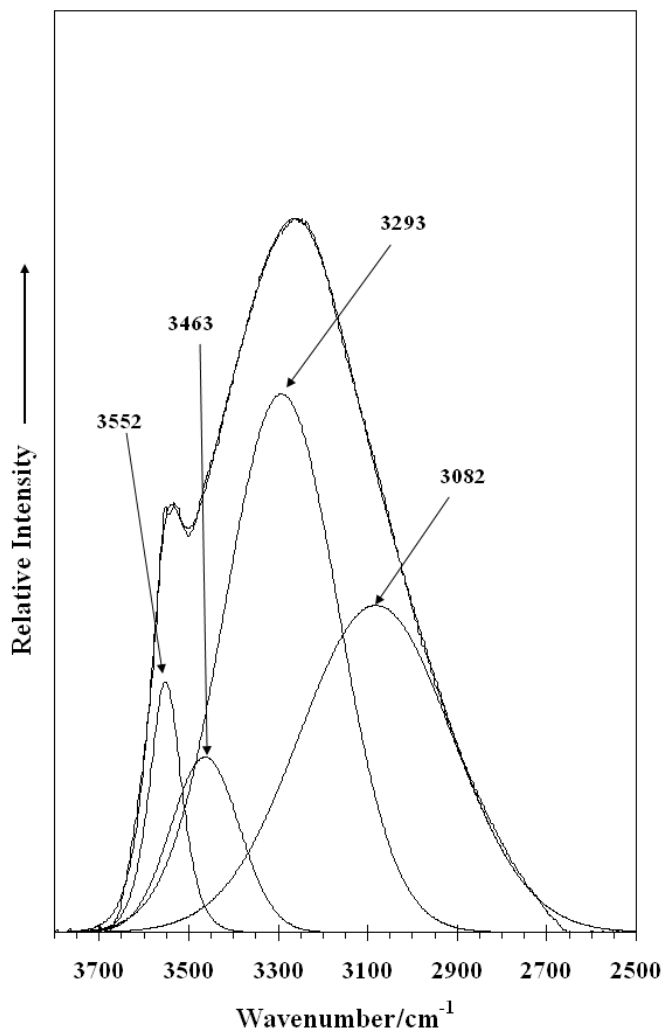
318

319

320 **Figure 4**

321

322



323

324

325 **Figure 5**